Apoptosis (2012) 17:236–247
DOI 10.1007/s10495-011-0672-3

ORIGINAL PAPER

Pleomorphic adenoma gene-like 2 regulates expression of the p53 family member, p73, and induces cell cycle block and apoptosis in human promonocytic U937 cells

Tracey S. Hanks · Katherine A. Gauss

Published online: 11 November 2011
© Springer Science+Business Media, LLC 2011

Abstract The proto-oncogene, pleomorphic adenoma gene-like 2 (PLAGL2), is implicated in a variety of cancers including acute myeloid leukemia (AML), malignant glioma, colon cancer, and lung adenocarcinoma. There is additional evidence that PLAGL2 can function as a tumor suppressor by initiating cell cycle arrest and apoptosis. Interestingly, PLAGL2 has also been implicated in human myelodysplastic syndrome, a disease that is characterized by ineffective hematopoiesis and can lead to fatal cytopenias (low blood counts) as a result of increased apoptosis in the marrow, or, in about one-third of cases, can progress to AML. To gain a better understanding of the actions of PLAGL2 in human myeloid cells, we generated a stable PLAGL2-inducible cell line, using human promonocytic U937 cells. PLAGL2 expression inhibited cell proliferation which correlated with an accumulation of cells in G1, apoptotic DNA-laddering, an increase in caspase 3, 8, and 9 activity, and a loss of mitochondrial transmembrane potential. There was significant increase in the p53 homologue, p73, with PLAGL2 expression, and consistent with mechanisms of p73-regulated cell cycle control and apoptosis, there was increased expression of known p73 target genes p21, DR5, TRAIL, and Bax. PLAGL2-induced cell cycle block was abolished in the presence of p73 siRNA. Together, these data support a role for PLAGL2 in cell cycle regulation and apoptosis via activation of p73.

Keywords PLAGL2 · p73 · Oncogene · Tumor suppressor · Cell cycle · Apoptosis

Introduction

Pleomorphic adenoma gene-like 2 (PLAGL2), along with PLAG1 and PLAGL1, belong to the small PLAG family of zinc-finger transcription factors [1]. PLAG proteins are highly homologous in the N-terminal zinc finger domain (PLAGL1 and PLAGL2 are 73 and 79% identical to PLAG1, respectively) with the C-terminal region being more divergent [2]. Considering the degree of identity between the zinc-finger DNA-binding domains, it is not surprising that PLAG proteins recognize similar GC rich consensus DNA-binding sequences, and raises the possibility that these family members regulate an overlapping set of target genes and pathways [3].

PLAG1 is considered an oncogene due to its involvement in the t(3:8)(p21; q12) chromosomal translocation associated with human pleomorphic adenomas of the salivary glands and increased expression in lipoblastomas and hepatoblastomas [4–7]. PLAGL1 inhibits tumor cell growth by controlling apoptosis and cell cycle progression, suggesting PLAGL1 functions as a tumor suppressor [8]. Interestingly, PLAGL2 has been shown to have both oncogenic and tumor suppressor activities. Like PLAGL1, PLAGL2 can induce cell cycle block and apoptosis. Overexpression of mouse PLAGL2 in Balb/c3T3 fibroblasts and neuroblastoma Neuroa2a cells caused an increase in the pro-apoptotic factor, bNip3, followed by apoptosis [9, 10]. In addition, cell injury and/or death in mouse lung epithelium were caused directly by PLAGL2-induced expression of bNip3 or indirectly by the aberrant expression of SP-C-induced endoplasmic reticulum stress [11].

Electronic supplementary material The online version of this article (doi:10.1007/s10495-011-0672-3) contains supplementary material, which is available to authorized users.

T. S. Hanks · K. A. Gauss (✉)
Department of Immunology and Infectious Diseases, Montana State University, 960 Technology Blvd., Bozeman, MT 59718, USA
e-mail: kgauss@montana.edu

In contrast, increased levels of PLAGL2 have implicated this family member in a variety of cancers. Amplification of the chromosomal region 20q11.21 containing PLAGL2 identified this family member as a suspect cancer gene in human malignant gliomas and colon cancer, and it was demonstrated that PLAGL2 inhibited neural stem cell differentiation and promoted self-renewal, partially through Wnt/β-catenin signaling [12]. Mouse models have also suggested a role for PLAGL2 in the development of lung adenocarcinoma and acute myeloid leukemia (AML) [13, 14]. Although the mechanism of PLAGL2-induced lung oncogenesis is not completely understood, PLAGL2 transgenic mice did show an increase in epithelial cells expressing SP-C, suggesting a role for PLAGL2 in the expansion of SP-C expressing cells. PLAGL2 was also identified as a cooperating oncogene in an inv(16) AML mouse model and was shown to be preferentially increased in human inv(16) AML samples [14]. Subsequently, it was demonstrated that PLAGL2 upregulated the thrombopoietin receptor Mpl in inv(16) AML mice, however, there was no correlation between PLAGL2 and Mpl expression in gene expression data sets of human AML [15].

Amplification of 20q11.21 was also observed in a number of human myelodysplastic syndrome (MDS) cases [16]. MDS is comprised of a heterogeneous group of clonal disorders characterized by inefficient hematopoiesis, and is considered a pre-leukemic condition, which can progress to AML [17]. MDS patients initially present with severe anemia, and as the disease worsens, they can develop fatal cytopenias due to increased apoptosis in the marrow, or, in 30–40% of cases, they develop AML. Although the mechanism of MDS to AML transition is not completely understood, the frequent association of chromosomal abnormalities with MDS suggests the involvement of an oncogene or a tumor suppressor in the pathogenesis and progression of the disease.

The opposing actions of PLAGL2 and the variable mechanisms of PLAGL2-induced oncogenesis suggest that PLAGL2 actions may be determined, in part, through cell or tissue specific modulators. Although PLAGL2 has been implicated in the pathogenesis of MDS and AML, to our knowledge almost nothing is known regarding the effects of PLAGL2 expression in human myeloid cells. Focusing on this, we generated a PLAGL2-inducible promonocytic U937 cell line, and for comparison, a non-myeloid cell line using human embryonic kidney cells (HEK293). PLAGL2 expression induced cell cycle block and apoptosis, similar to the effects observed in PLAGL1-expressing LLC-PK1 and SaOs-2 cells [8]. We show significant increase in the p53 homologue, p73, as well as activation of known p73 target genes, suggesting a novel mechanism for PLAGL2 regulation of cell cycle and apoptosis in human myelomonocytic cells.

Materials and methods

Reagents

Oligonucleotide primers were synthesized by Integrated DNA Technologies, and antibodies were from Santa Cruz (p57, #sc-1040; p27, #sc-528; p21, #sc-397; Bcl-2, #sc-783; Bid/tBid, #sc-11423; DR3, #sc-7909; DR5, #sc-53688), Proteintech Group, Inc (PlagL2, #11540-1-AP), Abcam (Tap73, #ab40658; ΔNp73, #ab13649; p53, #ab1101), and Cell Signaling (Bax, #2774; GAPDH, #2118).

Stable, PLAGL2-inducible cell lines

The HEK293 Tet-On PLAGL2 cell line (HEK293-PLAGL2) was made using the Tet-On Advanced Inducible Gene Expression System from Clontech (#630930) as follows. Full length PLAGL2 cDNA was cloned into the *Eco*RI/*Bam*HI restrictions sites in the multiple cloning site of pTRE-tight vector and the recombinant plasmid, pTRE-Tight-PLAGL2, was sequenced for integrity. pTRE-Tight-PLAGL2 (8 μg) and the Linear Hygromycin Marker (400 ng) were transfected into 10^6 HEK293 Tet-On cells (Clontech, #630903) using Lipofectamine 2000 (Invitrogen, #11668) according to the manufacture's protocol. Hygromycin (200 μg/ml) was added to cultures 24 h post-transfection and media containing G418 (100 μg/ml) and hygromycin was replaced every 4 days until large colonies were visible. Ten to 20 colonies were isolated using cloning discs, expanded in selection media, and screened for PLAGL2 expression as follows. Cells were treated with 1000 ng/ml doxycycline for 48 h to induce PLAGL2 expression and cell lysates were subjected to α-PLAGL2 Western blot analysis as previously described [18]. PLAGL2 positive clones were expanded and maintained in selection media.

U937 cells are a myelomonocytic cell line derived from a patient with histocytic lymphoma [19, 20]. The U937 Tet-Off PLAGL2 cell line (U937-PLAGL2) was generated by transfecting 10^6 promonocytic U937 Tet-Off cells [21] (a kind gift from Dr. Thomas Pabst) with 3 μg of pTRE-Tight-PLAGL2 and 300 ng of the Linear Hygromycin Marker using electroporation (Amaxa nucleofector, solution V, program W-001) according to the manufacturer's suggestion. After 24 h, cells were recovered by centrifugation, resuspended in selection media containing G418 (300 μg/ml), hygromycin (200 μg/ml), and tetracycline (1000 ng/ml) and plated using ClonaCell-TCS medium (STEMCELL, #03814). Drug resistant colonies were expanded and clones were analyzed for PLAGL2 expression by removal of tetracycline with 2 × 50 ml PBS washes, incubating cells for an additional 48 h, and subjecting cell lysates to α-PLAGL2 Western blot analysis. PLAGL2 positive clones were expanded and maintained in selection media.

Quantitative reverse transcriptase-polymerase chain reaction (qRT-PCR)

HEK293-PLAGL2 and U937-PLAGL2 cells were treated to induce PLAGL2 expression by the addition of doxycycline or the removal of tetracycline, respectively. 24 or 48 h post-induction, total RNA was isolated using the RNeasy mini kit (Qiagen, #74106) and subjected to qRT-PCR using PLAGL2, bNip-3, or SP-C specific QuantiTect Primers and QuantiTect SYBR Green RT-PCR kit (Qiagen, #204243) following the manufacturer's suggestion. Plus and minus induced samples were run on an ABI 7500 Fast System and results analyzed using the ABI 7500 System SDS software. All samples were run in triplicate.

Cell proliferation

HEK293-PLAGL2 and U937-PLAGL2 cells were plated on day 0 and treated with doxycycline (HEK293) or by removing tetracycline (U937). Every 24 h cells were analyzed using AlamarBlue (Invitrogen, #DAL1025) as suggested by the manufacture. Briefly, AlamarBlue was added to the cells, incubated for 4 h, and fluorescence was read using 555EX nm/585EM nm filter settings using the Flexstation II (Molecular Devices). Cell numbers were also determined and shown to directly correlate with the AlamarBlue fluorescence data.

Cell cycle analysis

HEK293-PLAGL2 and U937-PLAGL2 cells were treated to induce PLAGL2 expression. Cell cycle analysis was performed using a 5-bromo-2′-deoxyuridine (BrdU) flow cytometry kit with a FITC labeled antibody detecting incorporated BrdU (BD Pharmigen, #559619) as described by the manufacturer. Briefly, cells were labeled with BrdU for 45 min then fixed and stored at −80°C. Thawed cells were permeabilized, fixed, treated with DNase, and treated with FITC-anti BrdU and 7-AAD, to indicate cells in S phase and stain DNA, respectively. Fluorophore uptake was measured on a FACS LSR (BD Pharmigen) using Diva software (BD Pharmigen) and plots were generated with DNA (PE-Cy 5-A) on the X axis and BrdU uptake (AlexaFluor 488-A) on the Y axis. Gates were set for G1, S, G2/M, and apoptotic fractions and percents were calculated as a fraction of the total cell population.

Apoptotic DNA-laddering

HEK293-PLAGL2 and U937-PLAGL2 cells were treated to induce PLAGL2 expression. At the indicated times, cells were lysed in 100 μl lysis buffer (1% NP40, 20 mM EDTA, 50 mM Tris–HCl, pH 7.5) for 10 s, spun for 5 min at 3000 rpm, and supernatant was transferred to a clean tube. 10 μl of 10% SDS and 10 μl of 50 mg/ml RNase A was added and incubated at 56°C for 2 h. 10 μl of 25 mg/ml Proteinase K was added and incubation continued for 2 h at 37°C. Chromatin fragments were precipitated from the supernatants with 10 M ammonium acetate (1/2 volume) and ice cold EtOH (2.5 volume) for 1 h at −80°C, spun 20 min maximum rpm, washed in 80% ethanol, dried, and resuspended in TE buffer. Four to 5 μg of DNA was run on a 2% agarose gel, stained with ethidium bromide, and visualized under UV light.

FITC Annexin V staining

Cells were washed twice with cold PBS and twice with binding buffer (10 mM HEPES, 140 mM NaCl, 2.5 mM $CaCl_2$, pH 7.4) and resuspended in 100 μl binding buffer and 5 μl Annexin V-FITC (BD Pharmingen, #556419). Samples were incubated for 15 min at RT (25°C) in the dark and viewed using a fluorescence microscope to detect FITC labeling.

Caspase activity

U937-PLAGL2 cells were treated to induce PLAGL2 expression. Caspase 3, 8, and 9 activity was measured every 24 h using the caspase colorimetric assay kits from BioVision (Caspase 3, #K106: Caspase 8, #K113: Caspase 9, #K1190) following the manufacturer's instruction on the Flex Station II (Molecular Devices). Fold induction of caspase activity was determined by dividing caspase activity in PLAGL2-expressing samples by activity in non-expressing samples after background subtraction.

Mitochondrial transmembrane potential (MTP)

U937-PLAGL2 cells were treated for PLAGL2 induction or not induced. The MitoCapture kit (BioVision, # K250) was used to assess the shift of the cell population to a decreased intensity of red fluorescence indicating disruption of mitochondrial potential, an early event defining apoptosis. Briefly, cells were resuspended with the Mitocapture reagent at 1 ul/ml, incubated for 15–20 min, and then analyzed by flow cytometry with cell counts on the Y axis and red fluorescence (PE-A) on the X axis.

To inhibit mitochondrial depolarization, cells were treated at 24 h with 150 μM 4,4′-diisothiocyanatostilbene-2,2′-disulfonic acid (DIDS) (Oakwood Products, Inc, #018566) and grown for an additional 48 h (72 h total). Cells were treated as above to detect mitochondrial membrane potential and analyzed by flow cytometry with cell

counts on the y axis and red fluorescence (PE-A) on the X axis. Dot plots of side scatter area (SSC-A) versus forward scatter area (FSC-A) demonstrate apoptotic (smaller, more granular) and normal (larger, less granular) cell populations, respectively.

Apoptosis arrays

U937 cells were induced or not induced for PLAGL2 expression and total protein or RNA was isolated for screening an Apoptosis Antibody Array (RayBiotech, #AAH-APO) or an Apoptosis RT Profiler PCR Array (SABiosciences, #PAHS-012C-2), respectively, according to the manufacturer's instruction. Changes in protein levels for the protein arrays were determined using densitometry of duplicate spots. Fold regulation for the PCR arrays was calculated using SABiosciences PCR Array Data Analysis software. Both the protein and PCR arrays, plus and minus PLAGL2 expression, were done in duplicate.

Reactive oxygen species (ROS) detection

ROS levels were determined by treating cells with 6-carboxy-2′,7′-dichlorodihydrofluorescein diacetate, di (acetoxymethyl ester) as per the manufacturer's suggestions (Invitrogen, #C-2938). Briefly, cells were harvested, resuspended in PBS containing 5 mM of probe, and incubated at 37°C for 60 min. Probe solution was removed and cells were resuspended in growth media for 60 min, followed by analysis using the Flex Station II (Molecular Devices).

ROS levels were also detected using the Diogenes Cellular Luminescence Enhancement System (National Diagnostics, #CL-202) as follows. Cells (2.5×10^5) were resuspended in 100 µl Diogenes Complete Enhancer Solution and luminescence read using a Fluoroskan Ascent FL (Labsystems).

Western blot analysis

HEK293-PLAGL2 and U937-PLAGL2 cells were treated for PLAGL2 induction or not induced. Protein was isolated and subjected to SDS-PAGE as previously described [18]. Briefly, equal amounts of samples were separated by SDS-PAGE on 10 or 12% polyacrylamide gels and transferred to nitrocellulose membrane. Prestained molecular weight standards (BioRad or Thermo Scientific) were included on all gels for reference. The appropriate antibodies were used to probe Western blots, followed by an HRP-conjugated secondary antibody (BioRad or Thermo Scientific). Chemiluminescent developed blots were analyzed using a FluorChem FC2 imager (Alpha Innotech).

siRNA knockdown

HEK293-PLAGL2 cells were transfected with Dharmacon siRNA using DharmaFECT transfection reagent (Dharmacon, #T-2001) as per the manufacturer's instructions as follows. Cells (2×10^5) were plated 24 h prior to transfection in 2 ml of antibiotic free medium in 6 well plates. Cells were transfected with 75 nM of siGLO (control) or p73 siRNA, or no siRNA (mock transfection). Two days post-transfection, media was replaced and samples were treated with doxycycline for PLAGL2 expression. After 3 days, cells were harvested for protein expression and cell cycle analysis.

U937-PLAGL2 cells were transfected using Dharmacon Accell siRNA as follows. Cells were plated in 6 well plates at 2×10^5 cells/ml in Accell siRNA delivery medium plus 1% fetal bovine serum. siRNA (none, siGLO, or p73 siRNA) was added to a final concentration of 2 µM/well. 48 h post transfection, cells were washed 3× in PBS and resuspended in fresh Accell siRNA medium with or without tetracycline to induce PLAGL2. After 72 h cells were harvested for protein expression and cell cycle analysis.

Statistical analysis

Paired *t*-tests and one-way ANOVA was performed on the indicated sets of data. Post-test analysis used Tukey's pairwise comparisons (GraphPad Prism Software, San Diego, CA). Pair-wise comparisons with differences at $P < 0.05$ were considered to be statistically significant.

Results

We generated U937-PLAGL2 (Tet-Off) and HEK293-PLAGL2 (Tet-On) stable, inducible cell lines as described in materials and methods. Figure 1 shows induction of PLAGL2 mRNA and protein by addition of doxycycline to HEK293-PLAGL2 cells or removal of tetracycline from U937-PLAGL2 cells. Twenty-four hr post-induction, QRT-PCR and Western blot analysis was used to determine optimal amounts of doxycycline and tetracycline for PLAGL2 induction (Fig. 1a, b). U937-PLAGL2 cells produced more PLAGL2 protein compared to HEK293-PLAGL2 cells (Fig. 1b), and at doxycycline concentrations greater than 1000 ng/mL, HEK293-PLAGL2 cells did not express increased levels of PLAGL2 (data not shown).

To determine the effects of PLAGL2 expression on cell growth, cell viability was assayed using AlamarBlue. As seen in Fig. 1c, both cell lines showed a decrease in cell viability with PLAGL2 expression, with a greater effect in U937-PLAGL2 cells. Even at the highest PLAGL2 expression levels (1000 ng/ml doxycycline), the HEK293-

PLAGL2 cells showed a reduction in cell viability that was similar to that observed in U937-PLAGL2 cells with much less PLAGL2 protein (10 ng/ml tetracycline). Cell numbers were determined and confirmed the lack of cell growth in these samples (data not shown). These results show that PLAGL2 expression inhibits cell growth in U937 and HEK293 cells.

PLAGL2 induces apoptosis and cell cycle block

As mentioned previously, the PLAG family member, PLAGL1, and the mouse homologue of human PLAGL2, are known to induce apoptosis and cell cycle arrest. Visual inspection of U937-PLAGL2-expressing cells in culture (Online Resource 1A), but not HEK293-PLAGL2

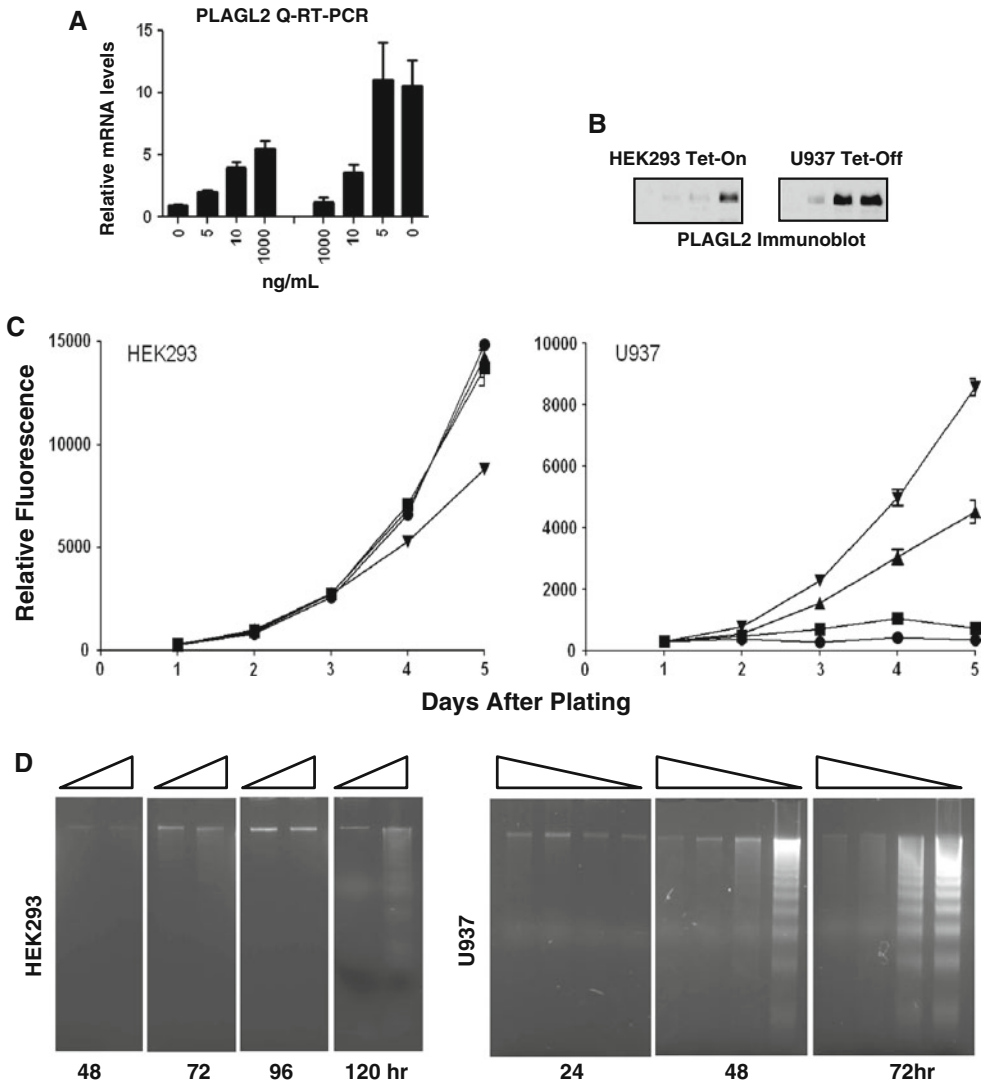

Fig. 1 PLAGL2 expression inhibits cell growth and induces DNA-laddering. **a** PLAGL2 qRT-PCR. **b** PLAGL2 immunoblot of PLAGL2-expressing HEK293 (Tet-On) and U937 (Tet-Off) cells. Cells were treated with doxycylcine (HEK293) or tetracycline (U937), at the concentrations indicated, to induce PLAGL2 expression. Total RNA or protein was isolated and analyzed by PLAGL2 qRT-PCR or PLAGL2 immunoblot 24 h post-induction, respectively. **c** PLAGL2 expression inhibits cell growth**.** HEK293- (*left*) and U937-PLAGL2-expressing (*right*) cells were plated on day 0 and treated with 0 (*circle*), 5 (*square*), 10 (*triangle*), or 1000 ng (*inverted triangle*) of doxycycline (HEK293) or tetracycline (U937) as indicated. Every 24 h AlamarBlue was added to the cells, incubated for 4 h, and fluorescence was read using 550EX nm/585EM nm filter settings using the Flex station II. These data are representative of at least three experiments. **d** PLAGL2 induces DNA-laddering. HEK293-PLAGL2 cells were treated for PLAGL2 expression with increasing amounts of doxycycline (0 and 1000 ng/ml), and U937-PLAGL2 cells were treated with decreasing amounts of tetracycline (1000, 10, 5, and 0 ng/ml) as indicated by the *triangle* over each gel. At the indicated times, cells were lysed, and chromatin fragments were precipitated from the supernatants. Four to 5 μg of DNA was run on a 2% agarose gel, stained with ethidium bromide, and viewed under UV light. These data are representative of two experiments

cells (data not shown), showed a steady increase in cell death over time, with the majority of cells (>80%) dead by day 5 post-induction. These results were confirmed by Trypan Blue staining (data not shown). DNA-laddering of chromatin, an indicator of apoptotic cell death, was analyzed to determine if PLAGL2-induced cell death was through an apoptotic mechanism. Figure 1d shows significant DNA-laddering in U937-PLAGL2-expressing cells by 48 h at the highest PLAGL2 expression level and at the two highest levels by 72 h, consistent with the cell viability assay (Fig. 1c). In addition, there was significantly more Annexin staining of U937-PLAGL2-expressing cells at 48 h when compared to the non-induced control (Online Resource 1B). There was only minimal DNA-laddering observed in the HEK293-PLAGL2-expressing cells at 120 h, possibly due to lower levels of PLAGL2 protein in these cells. These data show that PLAGL2 induces apoptosis in U937-PLAGL2-expressing cells and suggest that apoptosis is initiated between 24 and 48 h.

FACS analysis of HEK293- and U937-PLAGL2-expressing cells was used to further characterize the effects of PLAGL2 expression on apoptosis and cell cycle progression. Initial studies detected no significant block in cell cycle at 24 h (data not shown), therefore, cells were induced for PLAGL2 expression and stained for DNA content and BrdU incorporation to indicate cell cycle phase and DNA synthesis, respectively, at 48, 72, and 96 h. Figure 2a shows FACS data at 72 h and Table 1 contains the percent of cells in each phase of the cell cycle at each time point. U937-PLAGL2-expressing cells showed an accumulation of cells in G1 ($\sim$23%), and to a lesser degree in G2/M ($\sim$7%), with a corresponding loss of cells in S phase compared to non-induced samples. In addition, there was an increase in the Sub-G1 (apoptotic) population compared to non-induced cells at 72 and 96 h of 3 and 6%, respectively. In contrast, while HEK293-PLAGL2-expressing cells also showed an accumulation of cells in G1 ($\sim$8–9%) which corresponded to a similar loss of cells in S phase, it was to a lesser degree, and there was no change in the Sub-G1 population. The data show that, while U937-PLAGL2 cells show a greater accumulation of cells in G1, and to a lesser extent in G2, as well as induced apoptosis, HEK293-PLAGL2 cells show less of a block in G1 with no change in the apoptotic fraction. Again, the dissimilarity in PLAGL2 expression levels between cell lines could account for the difference in response. In addition, the inability to detect a block in the cell cycle at 24 h and the significant block observed in G1 by 48 h in both cell lines, suggests that the block in cell cycle is initiated between 24 and 48 h, similar to induction of apoptosis.

PLAGL2 expression induces the caspase cascade and a loss of MTP

Because PLAGL2-induced apoptosis in mouse cells was shown to be via bNip-3 and/or SP-C [11], we used qRT-PCR to look for changes in mRNA levels for these genes. There were no PLAGL2-induced changes in bNip-3 or SP-C mRNA levels in HEK293- or U937-PLAGL2-expressing cells (Online Resource 2), suggesting that the PLAGL2-induced apoptosis in U937 cells is via a different mechanism.

We have shown previously that PLAGL2 regulated expression of $p67^{phox}$, a protein component of the nicotinamide adenine dinucleotide phosphate (NADPH) oxidase complex, and was required for increased NADPH oxidase activity in response to TNF-α [22]. Because the NADPH oxidase can be activated in U937 cells to produce ROS, and ROS can induce apoptosis [23], we analyzed ROS levels in response to PLAGL2 expression. U937-PLAGL2 cells induced for PLAGL2 expression were treated with ROS detection reagent, 6-carboxy-2′,7′-dichlorodihydrofluorescein diacetate, di (acetoxymethyl ester) (Online Resource 3A). There was basal ROS production detected in non-induced cells (-PLAGL2), but no measurable increase in ROS levels in PLAGL2-expressing cells at 48 or 72 h. To rule out undetected subtle changes in ROS, we assayed for O_2^- production using the more sensitive (100–600 fold) Diogenes cellular luminescence enhancement system. While there were no changes in O_2^- levels in the presence of PLAGL2 at 24 h, there was a slight increase at 72 h when comparing ± PLAGL2 expressing cells (Online Resource 3B). However, detection of DNA laddering, as well as increased Annexin V staining and caspase activity, prior to 72 h suggested that the mechanism of PLAGL2-induced apoptosis was not via increased levels of ROS.

Next we asked if PLAGL2-induced apoptosis involved the caspase cascade. U937-PLAGL2 cells were treated for PLAGL2 expression and cell lysates were assayed for initiator caspase 8 and 9 and effector caspase 3 activity every 24 h over 4 days (Fig. 2b). There was a statistically significant increase in caspase 3 and 9 activity by 48 h and caspase 8 by 72 h, demonstrating that PLAGL2 expression activates the caspase cascade.

To determine if PLAGL2-induced apoptosis is through the extrinsic or intrinsic apoptotic pathways, we determined if PLAGL2 expression caused a loss of MTP (Online Resource 4). While there was a loss of MTP observed with PLAGL2 expression (Online Resource 4A), there was no change in the percent of apoptotic cells when samples were treated with DIDS, a mitochondrial anion channel inhibitor (Online Resource 4B). Together, these

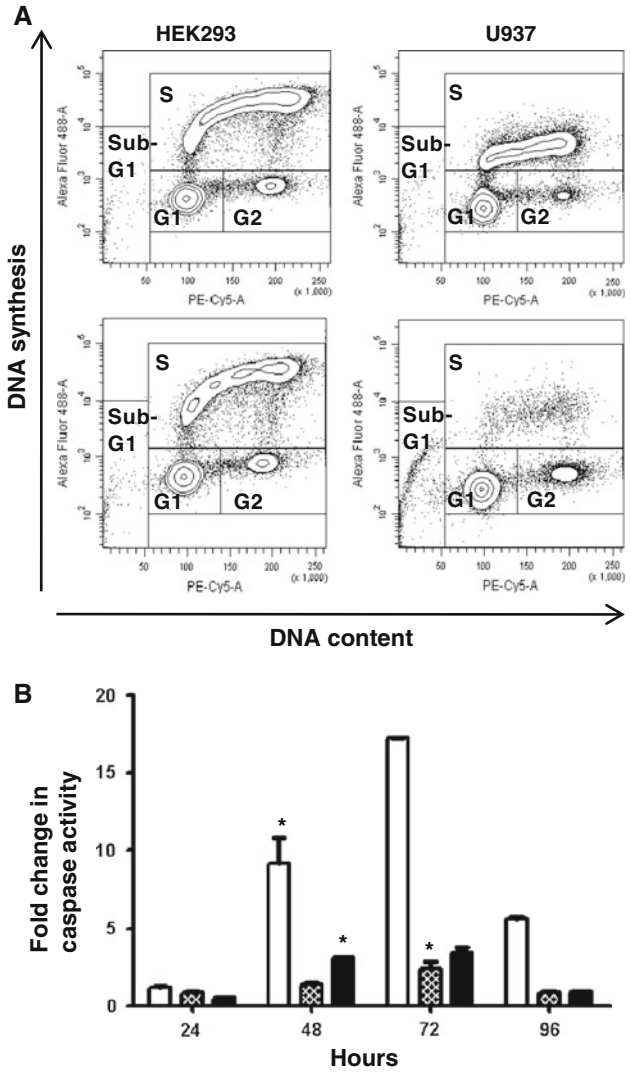

Fig. 2 PLAGL2 expression causes cell cycle block and activates the caspase cascade. **a** PLAGL2-induced cell cycle block. HEK293-PLAGL2 and U937-PLAGL2 cells were treated to induce PLAGL2 expression. At 48, 72, and 96 h cells were harvested and treated with BrdU followed by incubation with a FITC labeled anti-BrdU antibody to detect cells in S phase, and stained with 7-AAD to detect DNA. Shown are representative FACS plots at 72 h. Fluorophore uptake was measured on a FACS LSR (BD) using Diva software (BD) and plots were generated with DNA content (PE-Cy 5-A) on the *X* axis and BrdU uptake (AlexaFluor 488-A) on the *Y* axis. Gates were set for Sub-G1, G1, S, and G2/M fractions and labeled as Sub-G1, G1, S, and G2, respectively. Percent of cells in each gate was calculated as a fraction of the total cells and shown in Table 1. *Upper panels* are non-induced and *lower panels* are PLAGL2-induced samples. These data are representative of at least three experiments. **b** PLAGL2 activates the caspase cascade. U937-PLAGL2 cells were induced for PLAGL2 expression, or not induced, and analyzed for caspase 3 (*open bar*), 8 (*hatched bar*), and 9 (*solid bar*) activity every 24 h using the caspase colorimetric assay kits from BioVision. Fold induction of caspase activity was determined by dividing caspase activity in PLAGL2-expressing samples by activity in non-expressing samples at each time point, after subtracting background. These data are representative of at least three experiments. $*P < 0.05$ compared to 24 h samples

data suggest that, while the mitochondrial apoptotic pathway is activated with PLAGL2 expression, it is not the major mechanism of PLAGL2-induced apoptosis.

PLAGL2 regulates the p53 homologue, p73, and known p73 target genes

To further characterize the mechanism of PLAGL2-induced apoptosis and cell cycle block in U937 cells, we screened an Apoptosis Antibody Array (RayBiotech) and an Apoptosis RT Profiler PCR Array (SABiosciences). Results are shown in Online Resources 5 and 6. Of particular interest was the ~75 fold increase in p73 mRNA observed in the PCR array screen with PLAGL2 expression. p73 is a p53 family member, and like p53, can induce cell cycle arrest through regulation of cell cycle inhibitors p21 and p57 and apoptosis through activation of death receptors, Bax activation, and endoplasmic reticulum (ER) stress [24–26]. Consistent with p73-induced apoptotic mechanisms, we saw an increase in mRNA levels for the death receptors, DR5 and DR3, of 2.3- and 111-fold, respectively, and the DR5 ligand, TRAIL, of 5.2-fold, as well as a slight increase in Bax mRNA of 1.3 fold. Increased levels of p21 protein of 1.6-fold were also detected, consistent with the mechanisms of p73-induced cell cycle arrest.

There are multiple isoforms of p73 due to differential mRNA splicing and activation of alternate promoters [27]. While the transactivation proficient TAp73 shows pro-apoptotic effects, the transactivation deficient, amino-deleted ΔNp73 has an anti-apoptotic function and it is the relative levels of these isoforms that determine cell survival versus cell death [24]. Western blot analysis was used to evaluate changes in p73 protein levels in U937 cells in response to PLAGL2 expression, as well as HEK293 cells to possibly explain the difference in response to PLAGL2. As seen in Fig. 3, Western blot analysis of U937- and HEK293-PLAGL2 cells showed an increase in TAp73 with PLAGL2 expression compared to non-induced cells. While the HEK293-PLAGL2 non-induced cells had basal levels of TAp73, the non-induced U937-PLAGL2 cells had no detectable levels of TAp73 protein. ΔNp73 protein was also detected in HEK293- and U937-PLAGL2 cells, however, there were no changes in expression levels with PLAGL2 induction in HEK293 cells and a decrease in U937 cells. Because p73 and p53 regulate similar genes to induce cell cycle block and apoptosis, we also looked at levels of p53 protein and saw no change in the levels of p53 with PLAGL2 expression. These data demonstrate that PLAGL2 increases levels of the apoptotic TAp73 protein, and suggest that PLAGL2-induced apoptosis is via an increase in the relative ratio of TAp73/ΔNp73.

Table 1 Cell cycle distribution of PLAGL2 expressing cells

	Sub-G1	G1	S	G2/M
HEK293				
48 h (−)	1%	37%	52%	11%
48 h (+)	1	45	44	9
72 h (−)	<1	42	50	9
72 h (+)	<1	50	41	9
96 h (−)	1	43	51	5
96 h (+)	<1	52	41	7
U937				
48 h (−)	1	37	56	7
48 h (+)	1	63	18	19
72 h (−)	<1	52	42	6
72 h (+)	3	79	6	13
96 h (−)	<1	66	30	4
96 h (+)	6	83	4	7

− no PLAGL2, + PLAGL2 induced

Although the antibody apoptosis array showed no change in Bax protein, the PCR apoptosis array did show a minimal change in Bax mRNA (Online Resources 5 and 6). Therefore, because Bax is a known p73 target gene, we analyzed protein levels for Bax, as well as the mitochondrial proteins Bid and Bcl-2 by Western blot analysis. There was an increase in Bax and a decrease in Bcl-2 protein levels observed in response to PLAGL2 (Fig. 3), consistent with changes in their respective mRNA levels as indicated in the PCR apoptosis array. Consistent with caspase 8 activation, there was a decrease in Bid corresponding to an increase in truncated tBid. HEK293 cells had much lower levels of tBid compared to U937 cells, as indicated by the lengthy exposure time required to detect protein. This result is consistent with the barely detectable increase in DR5 levels in these cells. There was a significant increase in DR3, and to a lesser extent, DR5, in U937-PLAGL2 cells, again, consistent with the PCR apoptosis array data. Together, these data demonstrate that PLAGL2 expression activates the extrinsic apoptotic pathway as noted by increased protein levels of death receptors DR5 and/or DR3, activation of caspase 8, and truncation of Bid.

The apoptosis antibody array showed a clear increase in p21, a member of the pCip/Kip family of cell cycle inhibitors [28]. We had prior indications that PLAGL2 also upregulated another pCip/Kip cell cycle inhibitor, p57, in HEK293-PLAGL2 cells (unpublished data). Because TAp73 has been shown to regulate both of these genes [26, 29], changes in p21 and p57, as well as the third pCip/Kip family member, p27, were investigated using Western blot analysis. Interestingly, all three proteins showed increased levels in HEK293- and U937-PLAGL2-expressing cells (Fig. 3), with greater increases in p21 and p57 levels in

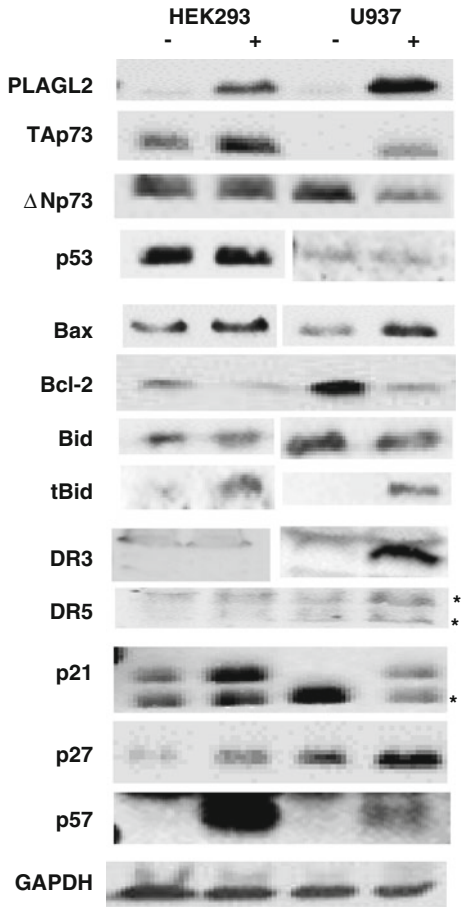

Fig. 3 PLAGL2 increases levels of TAp73 and known p73 target genes. HEK293- and U937-PLAGL2 cells were treated for PLAGL2 induction (+) or not induced (−) as indicated. Protein was isolated and equal amounts of protein were subjected to 10 or 12% SDS-PAGE followed by immunoblot analysis for the indicated proteins. Chemiluminescence was detected using a FluorChem FC2 imager. HEK293 tBid Western blot required lengthy exposures to detect protein. * indicates DR5 isoforms and truncated p21 [46]

HEK293 cells and a greater increase in p27 levels in U937 cells. These data suggest a role for PLAGL2-induced cell cycle block via TAp73 regulation of the pCip/Kip family of cell cycle inhibitors.

p73 knockdown inhibits PLAGL2-induced cell cycle block and Bax expression

To determine if PLAGL2 regulation of p73 caused cell cycle block and apoptosis, HEK-293- and U937-PLAGL2 cells were transfected with p73 siRNA. Figure 4a shows efficient knockdown of TAp73 protein in HEK293 cells to below basal levels after 72 h of siRNA treatment. While knockdown of p73 was observed in U937 cells, levels were still greater than those sufficient to induce apoptosis and cell cycle block at 48 h (Fig. 4a). The difference in the degree of p73 knockdown is likely due to poor transfection

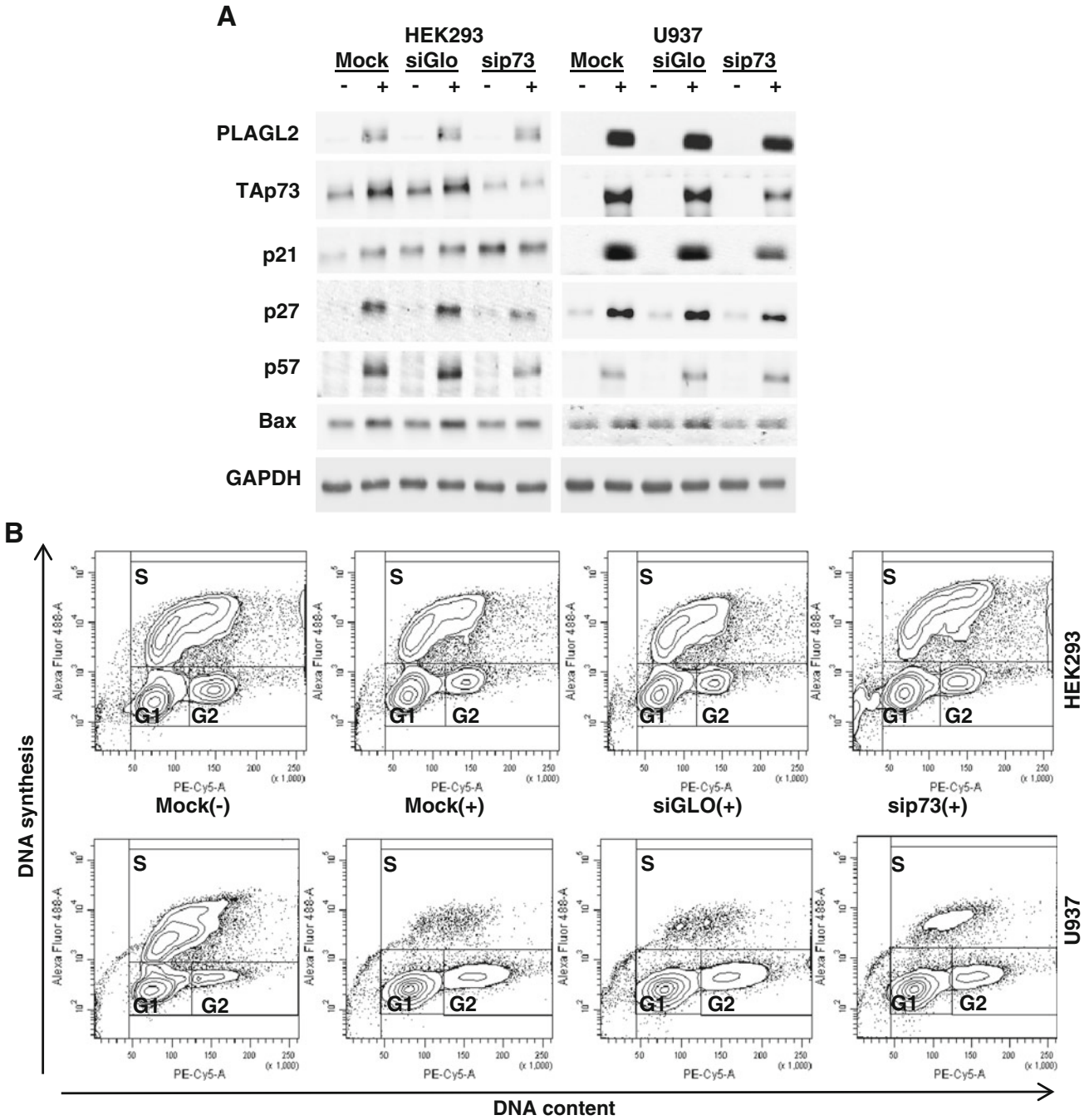

Fig. 4 p73 knockdown in HEK293-PLAGL2-expressing cells inhibits its PLAGL2-induced cell cycle arrest. **a** p73 knockdown in HEK293- and U937-PLAGL2 cells. HEK293- and U937-PLAGL2 cells were mock transfected or transfected with siGLO (negative control) or p73 siRNA. Cells were treated for PLAGL2 induction (+), or not induced (−) as indicated. Protein was harvested at 72 h post-induction. Equal amounts of protein were subjected to SDS-PAGE and analyzed by western blot for the indicated proteins. **b** p73 knockdown inhibits PLAGL2-induced cell cycle arrest. HEK293- and U937-PLAGL2 cells were mock transfected or transfected with siGLO (negative control) or p73 siRNA (sip73) as indicated. Cells were treated for PLAGL2 induction (+), or not induced (−) as indicated. 72 h post-induction cells were harvested for cell cycle analysis. Cells were labeled to detect S phase (*Y* axis) cells and DNA content (*X* axis) and analyzed as in Fig. 4. Percent of cells in each gate was calculated as a fraction of the total cells and shown in Table 2. *Upper panel* HEK293-PLAGL2-expressing cells, *lower panel* U937-PLAGL2-expressing cells

efficiency of U937 cells. PLAGL2-induced cell cycle block in HEK293 cells was completely inhibited in the presence of p73 siRNA as noted by similar cell cycle distribution when comparing mock transfected, non-induced cells and p73 siRNA PLAGL2-expressing cells (Fig. 4b, upper panel, and Table 2). This result is consistent with reduced

expression of cell cycle inhibitors p27 and p57, and to a lesser extent p21, in p73 siRNA HEK293-PLAGL2-expressing cells (Fig. 4a). Similar affects were observed with the U937 cells, although to a lesser degree, again, possibly due to inefficient p73 knockdown (Fig. 4b, lower panel, and Table 2). The decrease in cells in G1 (3%) was minimal when comparing mock transfected U937-PLAGL2-expressing cells to p73 siRNA treated PLAGL2-expressing cells with a consistent and corresponding increase in cells in S phase. While there was reduction in p21, the effect was less for p27 and there was no change in p57 levels. Due to ineffective p73 knockdown in U937 cells and the increase in the apoptotic population as a result of transfection alone (Table 2, Mock-), a direct role of p73 in PLAGL2-induced apoptosis in U937 cells could not be determined. We did, however, note a reduction in Bax protein with p73 siRNA treatment in both cell lines, demonstrating that PLAGL2 activation of p73 regulates expression of pro-apoptotic Bax. Together, the data show that PLAGL2 activation of p73 regulates cell cycle in HEK293, and suggests that PLAGL2-induced apoptosis in U937 cells may be, in part, regulated by p73 activation of pro-apoptotic Bax.

Discussion

Given the implication of PLAGL2 in the pathogenesis of MDS and AML [14–16], understanding the mechanisms of PLAGL2 actions in human myeloid cells may provide insights into the potential role of PLAGL2 in these blood diseases. The present study shows that PLAGL2-induced cell cycle block and apoptosis in the human myelomonocytic U937 cell line is not via bNip-3 or SP-C pathways as demonstrated in mouse Balb/c3T3 fibroblasts, neuroblastoma Neuroa2a cells and mouse lung epithelium [10, 11]. Rather, our data support a role for PLAGL2 in cell cycle regulation and apoptosis via activation of the p53 homologue, p73, and p73 target genes.

Table 2 Affect of p73 siRNA on cell cycle distribution

	Sub-G1	G1	S	G2/M
HEK293				
Mock (−)	3%	48%	37%	10%
Mock (+)	3	56	29	10
siGlo (+)	3	60	28	9
sip73 (+)	6	48	35	10
U937				
Mock (−)	3	48	42	8
Mock (+)	2	77	6	14
siGlo (+)	3	76	7	15
sip73 (+)	3	74	10	12

− no PLAGL2, + PLAGL2 induced

Cellular stresses such as oncogene expression and DNA damage can activate p73 and lead to growth arrest and apoptosis [24, 30]. Overexpression of oncogenes has been shown to activate p73 transcription, and in the case of E2F1, p73 activation is through direct binding of E2F1 to the p73 promoter [31–33]. Other studies have shown that cisplatin and ionizing radiation-induced DNA damage activates c-Abl kinase causing an accumulation of p73 through protein stabilization [34–36]. Additional proteins shown to regulate p73 activity through post-translational modifications or protein–protein interactions include acetyltransferase p300, MDM2, Itch, FBOX45, NEDL2, Cyclin G, UFD2a, and ASPP family of proteins [27]. The mechanism of PLAGL2-induced p73 activation was not determined in this study; however, the significant increase in TAp73 mRNA suggests that PLAGL2 expression affects p73 transcription. It is possible that, as a transcription factor, PLAGL2 regulates p73 expression through direct binding to the p73 promoter in a manner similar to E2F1. Another possibility is that, like other oncogenes, overexpression of PLAGL2 may cause DNA damage resulting in activation of p73 [37]. p73 can also be activated by increases in ROS levels [24], although our data suggests a different mechanism of activation in U937 cells. Additional studies are necessary to determine the mechanism of PLAGL2-induced p73 activation.

Alternative promoter utilization and alternative mRNA splicing give rise to a number of p73 isoforms that can act as transcription activators or inhibitors depending on the presence or lack of the transactivation domain (TA) [38–41]. While p73 isoforms do not interact with wild-type p53, mutated p53 associates with p73 to abrogate p73 function, and the ΔNp73 isoforms are capable of inhibiting transcriptional activity of both p73 and p53. In addition, different TAp73 isoforms can act differently depending on the tumor cell background [25]. For example, while the TAp73β isoform usually suppresses growth, interaction with the proto-oncogene c-Jun promotes cell survival [42]. Therefore, the ratio of specific TAp73/ΔNp73 isoforms and the status of p53, as well as intracellular content, play a role in regulating the apoptotic versus pro-survival activities of p73. Although we did not determine the specific isoform of TAp73 or ΔNp73 expressed in the cell lines tested here, we show that PLAGL2 expression increased the ratio of TAp73 to ΔNp73, therefore favoring the pro-apoptotic action of TAp73. In addition, the level and/or status of p53 may also play a role in p73 activity in response to PLAGL2 expression. It is worth noting that there is a third p53 family member, p63, and functional cross-talk between family members through homotypic and heterotypic interactions suggests that the relative levels of all three members may

determine the response of the p53 pathway in different cell types [43]. Further studies will be necessary to determine the role of p73 isoforms, p53 and p63 status, and cell type-specificity in PLAGL2-induced apoptosis.

Although we were not able to directly show PLAGL2-induced apoptosis was via p73 through siRNA knockdown, we clearly demonstrated activation of the extrinsic apoptotic pathway as seen by increased levels of protein and mRNA for DR5 and its ligand TRAIL, respectively, activation of caspase 8, and truncation of Bid to tBid. Considering that over-expression of PLAGL2 has been linked to a subset of MDS cases [16], it is interesting to note that pro-apoptotic cytokines, including the p73 target TRAIL, are believed to contribute to the increased frequency of apoptosis in MDS marrow [44]. While DR3 is not a known p73 target gene, there was a greater increase in DR3 mRNA and protein relative to DR5, suggesting that this death receptor may also play a role in PLAGL2-induced apoptosis. In addition, while caspase 8 can activate caspase 3 through the mitochondria via tBid, caspase 3 can also be activated directly by caspase 8. This could explain why maintaining mitochondrial membrane integrity with DIDS had no effect on apoptosis and suggests that the primary mechanism of PLAGL2-induced apoptosis is via activation of the extrinsic, death receptor apoptotic pathway. The strong apoptotic response in U937 cells compared to HEK293 cells could be explained by the relatively small increase in DR5 and tBid in HEK293 cells versus U937 cells and/or cell specific factors, including the relative ratios of pro-apoptotic versus pro-survival signals. We cannot rule out the possibility that the difference in response to PLAGL2 between the HEK293 and U937 cell lines is simply due to dissimilar levels of PLAGL2 expression and studies comparing different cell lines with comparable, inducible expression levels of PLAGL2 are needed to clarify this matter. In addition, future studies that take advantage of the heterogeneity of the p73- and p73 + siRNA U937 cells will be important to better evaluate the role of p73 in PLAGL2-induced apoptosis.

Consistent with p73 regulation of the cell cycle through activation of cell cycle inhibitors, we show that PLAGL2 induced G1 cell cycle block in HEK293- and U937-PLAGL2-expressing cells, and to a lesser extent, a G2/M block in U937 cells. PLAGL1 also induces cell cycle block, but only in G1, and depending on the cell type, may or may not involve p21 transcriptional regulation and p53 interactions [8, 45]. We report here that PLAGL2 also regulates expression of p21, as well as p27 and p57, in HEK293 and U937 cells. Together, these data support the notion that PLAG proteins regulate similar cellular processes via an overlapping set of target genes, and that cell specificity plays a role in the actions of PLAG proteins, potentially though cell specific cofactors and modulators.

In conclusion this report provides evidence supporting a role for PLAGL2 regulation of the cell cycle and apoptosis via activation of p73 and p73 target genes. It is interesting that PLAGL2 has both oncogenic and tumor suppressive activity, as does p73, and is implicated in both MDS and AML, diseases characterized by opposing phenotypes (cell death versus proliferation). Here we show that PLAGL2 activates several p73 target genes, including TRAIL, which is intriguing considering the potential link between PLAGL2 and MDS, and that increased levels of TRAIL in MDS likely contributes to the anemia in MDS cases through increased apoptosis in the marrow [44]. While it has not been definitively proven that PLAGL2 plays a role in the pathogenesis of MDS or AML, it appears that the microenvironment does affect PLAGL2 actions, likely through cell specific factors, and, as suggested by this study, potentially through PLAGL2 modulation of the ratio of cell-specific p73 isoforms and expression of p73 target genes. Future studies will be important to elucidate the mechanism of PLAGL2 activation of p73 and to identify cell specific factors that affect PLAGL2 actions to better understand the role of this PLAG family member in important cellular processes, such as cell cycle, apoptosis, and tumorigenesis.

Acknowledgments We thank Dr. Nicole Meissner and Dr. George Gauss for their critical reading of the manuscript. This work was supported by the National Institutes of Health Grant P20 RR-024237.

Conflict of interest The authors declare they have no conflict of interest.

References

1. Abdollahi A (2007) LOT1 (ZAC1/PLAGL1) and its family members: mechanisms and functions. J Cell Physiol 210:16–25
2. Kas K, Voz ML, Hensen K, Meyen E, Van de Ven WJM (1998) Transcriptional activation capacity of the novel PLAG family of zinc finger proteins. J Biol Chem 273:23026–23032
3. Hensen K, Van Valckenborgh IC, Kas K, Van de Ven WJ, Voz ML (2002) The tumorigenic diversity of the three PLAG family members is associated with different DNA binding capacities. Cancer Res 62:1510–1517
4. Kas K, Voz ML, Roijer E, Astrom AK, Meyen E, Stenman G et al (1997) Promoter swapping between the genes for a novel zinc finger protein and beta-catenin in pleiomorphic adenomas with t(3;8)(p21;q12) translocations. Nat Genet 15:170–174
5. Astrom A, D'Amore ES, Sainati L, Panarello C, Morerio C, Mark J et al (2000) Evidence of involvement of the PLAG1 gene in lipoblastomas. Int J Oncol 16:1107–1110
6. Hibbard MK, Kozakewich HP, Dal CP, Sciot R, Tan X, Xiao S et al (2000) PLAG1 fusion oncogenes in lipoblastoma. Cancer Res 60:4869–4872
7. Zatkova A, Rouillard JM, Hartmann W, Lamb BJ, Kuick R, Eckart M et al (2004) Amplification and overexpression of the IGF2 regulator PLAG1 in hepatoblastoma. Genes Chromosomes Cancer 39:126–137

8. Spengler D, Villalba M, Hoffmann A, Pantaloni C, Houssami S, Bockaert J et al (1997) Regulation of apoptosis and cell cycle arrest by Zac1, a novel zinc finger protein expressed in the pituitary gland and the brain. EMBO J 16:2814–2825
9. Furukawa T, Adachi Y, Fujisawa J, Kambe T, Yamaguchi-Iwai Y, Sasaki R et al (2001) Involvement of PLAGL2 in activation of iron deficient- and hypoxia-induced gene expression in mouse cell lines. Oncogene 20:4718–4727
10. Mizutani A, Furukawa T, Adachi Y, Ikehara S, Taketani S (2002) A zinc-finger protein, PLAGL2, induces the expression of a proapoptotic protein Nip3, leading to cellular apoptosis. J Biol Chem 277:15851–15858
11. Yang YS, Yang MC, Guo Y, Williams OW, Weissler JC (2009) PLAGL2 expression-induced lung epithelium damages at bronchiolar alveolar duct junction in emphysema: bNip3- and SP-C-associated cell death/injury activity. Am J Physiol Lung Cell Mol Physiol 297:L455–L466
12. Zheng H, Ying H, Wiedemeyer R, Yan H, Quayle SN, Ivanova EV et al (2010) PLAGL2 regulates Wnt signaling to impede differentiation in neural stem cells and gliomas. Cancer Cell 17:497–509
13. Yang YS, Yang MC, Weissler JC (2011) Pleiomorphic adenoma gene-like 2 expression is associated with the development of lung adenocarcinoma and emphysema. Lung Cancer. doi:10.1016/j.lungcan.2011.02.006
14. Landrette SF, Kuo YH, Hensen K, Barjesteh van Waalwijk van Doorn-Khosrovani S, Perrat PN, Van de Ven WJ et al (2005) Plag1 and Plagl2 are oncogenes that induce acute myeloid leukemia in cooperation with Cbfb-MYH11. Blood 105:2900–2907
15. Landrette SF, Madera D, He F, Castilla LH (2011) The transcription factor PlagL2 activates Mpl transcription and signaling in hematopoietic progenitor and leukemia cells. Leukemia 25:655–662
16. Mackinnon RN, Selan C, Wall M, Baker E, Nandurkar H, Campbell LJ (2010) The paradox of 20q11.21 amplification in a subset of cases of myeloid malignancy with chromosome 20 deletion. Genes Chromosomes Cancer 49:998–1013
17. Mhawech P, Saleem A (2001) Myelodysplastic syndrome: review of the cytogenetic and molecular data. Crit Rev Oncol Hematol 40:229–238
18. Wezensky SJ, Hanks TS, Wilkison MJ, Ammons MC, Siemsen DW, Gauss KA (2010) Modulation of PLAGL2 transactivation by positive cofactor 2 (PC2), a component of the ARC/Mediator complex. Gene 452:22–34
19. Sundstrom C, Nilsson K (1976) Establishment and characterization of a human histiocytic lymphoma cell line (U-937). Int J Cancer 17:565–577
20. Harris P, Ralph P (1985) Human leukemic models of myelomonocytic development: a review of the HL-60 and U937 cell lines. J Leukoc Biol 37:407–422
21. Boer J, Bonten-Surtel J, Grosveld G (1998) Overexpression of the nucleoporin CAN/NUP214 induces growth arrest, nucleocytoplasmic transport defects, and apoptosis. Mol Cell Biol 18:1236–1247
22. Ammons MC, Siemsen DW, Nelson-Overton LK, Quinn MT, Gauss KA (2007) Binding of pleomorphic adenoma gene-like 2 to the tumor necrosis factor (TNF)-alpha-responsive region of the NCF2 promoter regulates p67(phox) expression and NADPH oxidase activity. J Biol Chem 282:17941–17952
23. Simon HU, Haj-Yehia A, Levi-Schaffer F (2000) Role of reactive oxygen species (ROS) in apoptosis induction. Apoptosis 5:415–418
24. Ramadan S, Terrinoni A, Catani MV, Sayan AE, Knight RA, Mueller M et al (2005) p73 induces apoptosis by different mechanisms. Biochem Biophys Res Commun 331:713–717
25. Holcakova J, Ceskova P, Hrstka R, Muller P, Dubska L, Coates PJ et al (2008) The cell type-specific effect of TAp73 isoforms on the cell cycle and apoptosis. Cell Mol Biol Lett 13:404–420
26. Blint E, Phillips AC, Kozlov S, Stewart CL, Vousden KH (2002) Induction of p57(KIP2) expression by p73beta. Proc Natl Acad Sci USA 99:3529–3534
27. Zawacka-Pankau J, Kostecka A, Sznarkowska A, Hedstrom E, Kawiak A (2010) p73 tumor suppressor protein: a close relative of p53 not only in structure but also in anti-cancer approach? Cell Cycle 9:720–728
28. Besson A, Dowdy SF, Roberts JM (2008) CDK inhibitors: cell cycle regulators and beyond. Dev Cell 14:159–169
29. Schmelz K, Wagner M, Dorken B, Tamm I (2005) 5-Aza-2′-deoxycytidine induces p21WAF expression by demethylation of p73 leading to p53-independent apoptosis in myeloid leukemia. Int J Cancer 114:683–695
30. Stiewe T, Putzer BM (2001) p73 in apoptosis. Apoptosis 6:447–452
31. Zaika A, Irwin M, Sansome C, Moll UM (2001) Oncogenes induce and activate endogenous p73 protein. J Biol Chem 276:11310–11316
32. Stiewe T, Putzer BM (2000) Role of the p53-homologue p73 in E2F1-induced apoptosis. Nat Genet 26:464–469
33. Irwin M, Marin MC, Phillips AC, Seelan RS, Smith DI, Liu W et al (2000) Role for the p53 homologue p73 in E2F–1-induced apoptosis. Nature 407:645–648
34. Gong JG, Costanzo A, Yang HQ, Melino G, Kaelin WG Jr, Levrero M et al (1999) The tyrosine kinase c-Abl regulates p73 in apoptotic response to cisplatin-induced DNA damage. Nature 399:806–809
35. Agami R, Bernards R (2000) Distinct initiation and maintenance mechanisms cooperate to induce G1 cell cycle arrest in response to DNA damage. Cell 102:55–66
36. Yuan ZM, Shioya H, Ishiko T, Sun X, Gu J, Huang YY et al (1999) p73 is regulated by tyrosine kinase c-Abl in the apoptotic response to DNA damage. Nature 399:814–817
37. Halazonetis TD, Gorgoulis VG, Bartek J (2008) An oncogene-induced DNA damage model for cancer development. Science 319:1352–1355
38. Yang A, Kaghad M, Wang Y, Gillett E, Fleming MD, Dotsch V et al (1998) p63, a p53 homolog at 3q27–29, encodes multiple products with transactivating, death-inducing, and dominant-negative activities. Mol Cell 2:305–316
39. Irwin MS, Kaelin WG (2001) p53 family update: p73 and p63 develop their own identities. Cell Growth Differ 12:337–349
40. Benard J, Douc-Rasy S, Ahomadegbe JC (2003) TP53 family members and human cancers. Hum Mutat 21:182–191
41. Moll UM, Slade N (2004) p63 and p73: roles in development and tumor formation. Mol Cancer Res 2:371–386
42. Vikhanskaya F, Toh WH, Dulloo I, Wu Q, Boominathan L, Ng HH et al (2007) p73 supports cellular growth through c-Jun-dependent AP-1 transactivation. Nat Cell Biol 9:698–705
43. Collavin L, Lunardi A, Del SG (2010) p53-family proteins and their regulators: hubs and spokes in tumor suppression. Cell Death Differ 17:901–911
44. Campioni D, Secchiero P, Corallini F, Melloni E, Capitani S, Lanza F et al (2005) Evidence for a role of TNF-related apoptosis-inducing ligand (TRAIL) in the anemia of myelodysplastic syndromes. Am J Pathol 166:557–563
45. Liu PY, Chan JY, Lin HC, Wang SL, Liu ST, Ho CL et al (2008) Modulation of the cyclin-dependent kinase inhibitor p21(WAF1/Cip1) gene by Zac1 through the antagonistic regulators p53 and histone deacetylase 1 in HeLa Cells. Mol Cancer Res 6:1204–1214
46. Blundell R, Harrison DJ, O'Dea S (2004) p21(Waf1/Cip1) regulates proliferation and apoptosis in airway epithelial cells and alternative forms have altered binding activities. Exp Lung Res 30:447–464